

An Investigation of the Control Mechanism of Plasma Actuators in a Shock Wave-Boundary Layer Interaction

N. Webb¹, C. Clifford², and M. Samimy³

*Gas Dynamics and Turbulence Laboratory
Aeronautical and Astronautical Research Laboratories
The Ohio State University
2300 West Case Road
Columbus, OH 43235*

Shock Wave-Boundary Layer Interaction (SWBLI) induced separation control using Localized Arc Filament Plasma Actuators (LAFPA) is investigated. The freestream Mach number is 2.3 and the boundary layer is fully turbulent ($Re_{\theta_i} = 27,900$). The impinging oblique shock wave is generated by a 10° compression ramp. The reflected shock is displaced upstream by approximately one boundary layer thickness (~ 5 mm) by the LAFPA. The control objective was to exploit potential natural instabilities within the flow to manipulate the low frequency ($St \sim 0.03$) unsteadiness associated with the upstream region of the interaction. Parametric studies of the LAFPA's effects seemed to indicate that unsteadiness manipulation is not the primary control mechanism but suggest that boundary layer degradation through heating is rather the primary control mechanism. Further examination of the boundary layer and interaction has shown this hypothesis to be correct.

Nomenclature

H	= upstream boundary layer shape factor (δ^*/θ), subscript “i” indicates incompressible value
L_{int}	= interaction length (mm)
St	= Strouhal number, normalized frequency: fL_{int}/U_∞
St_F	= Strouhal number at which the actuators are operated
U_∞	= freestream velocity upstream of the interaction
X_o	= streamwise location of the projected primary shock inviscid impingement point
X^*	= normalized streamwise coordinate: $(X - X_o)/L_{int}$
X_a^*	= normalized streamwise location of the actuators
α	= compression ramp angle
δ	= upstream boundary layer thickness
δ^*	= upstream boundary layer displacement thickness, subscript “i” indicates incompressible value
θ	= upstream boundary layer momentum thickness, subscript “i” indicates incompressible value

I. Introduction

Shock Wave-Boundary Layer Interactions (SWBLIs) commonly occur in high-speed flows from the transonic to the hypersonic regime. They can be found in a variety of applications including transonic wings, axial turbines, and mixed-compression inlets. The interaction often results in performance detriments because the boundary layer must negotiate the imposed adverse pressure gradient. The effect of the pressure gradient on the low momentum regions of the boundary layer significantly degrades the incoming boundary layer, and, in severe cases, can cause separation. These effects (especially the increased unsteadiness and aerodynamic blockage associated with separation) have the potential to reduce system performance significantly. In the case of supersonic inlets, boundary layer bleed has often been used to, among other things, control SWBLI induced separation.^{1,2} Although bleed is effective, it has inherent efficiency penalties that make the minimization or elimination of bleed desirable.

¹ Graduate Student, Department of Mechanical and Aerospace Engineering, AIAA Student Member

² Graduate Student, Department of Mechanical and Aerospace Engineering, AIAA Student Member

³ John B. Nordholt Professor of Mechanical and Aerospace Engineering, AIAA Fellow, Email: samimy.1@osu.edu

Both passive and active control methods have been investigated as potential separation control techniques to replace bleed. A commonly studied passive technique is the use of vortex generators to diffuse momentum into the near wall region. A wide variety of vortex generator shapes and sizes have been studied by many research groups.³⁻⁷ Geometric modifications have also been studied as a means of changing the wave structure to reduce the intensity of the adverse pressure gradient.⁸ Although passive control techniques do not require external energy, active control methods can provide greater flexibility. Kalra et al.⁹ have investigated the use of magnetically driven arcs (magnetohydrodynamic discharge actuators) to inject momentum into the near wall region. Micro-jets^{10,11} and synthetic jets¹² have also been used as aerodynamic vortex generators, their primary advantage being greater flexibility than their physical counterparts. These types of active flow control have shown to have an effect on the separation size and intensity; however, the magnitude of the effect is invariably tied to the amount of energy used by the actuators, which can become prohibitive for high-speed applications.

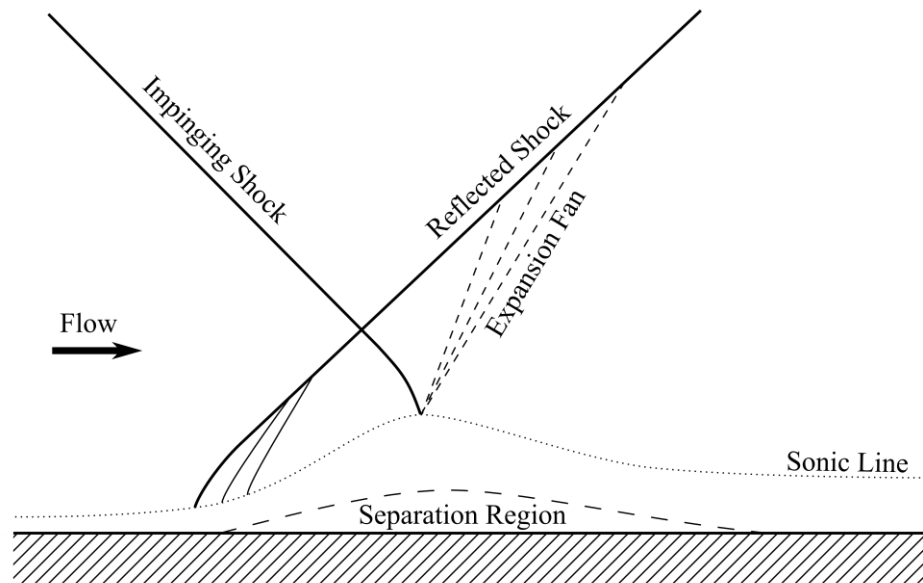


Figure 1: Schematic of an Impinging SWBLI with Flow Separation

By exploiting the ability of some flows to amplify introduced perturbations, active flow control can sidestep this issue by allowing the flow to amplify the input. Thus, by properly perturbing the flow, the desired effect can be obtained with relatively little external energy input. The instabilities responsible for amplifying introduced perturbations often cause unsteadiness in the baseline flow. Natural unsteadiness has long been observed and studied in SWBLIs, especially when separation is present. Low frequency, large amplitude unsteadiness of a broadband nature has been observed in the region around the foot of the reflected shock (see Figure 1).¹³⁻¹⁵ Effectively exploiting natural instabilities for flow control requires a good understanding of the nature of the instability. A review of the SWBLI literature reveals two primary positions on the source of unsteadiness: 1) Upstream perturbations cause the shock to oscillate at a low frequency, which causes the separation size to fluctuate. 2) The separation region periodically expands/contracts due to some other mechanisms (potentially an instability), which force the shock to oscillate. Researchers seeking evidence for the first theory usually attempt to correlate events, or instantaneous fluctuations in the boundary layer with shock movement/position^{16,17} or to examine the upstream boundary layer for structures which could cause such behavior.^{18,19} Researchers who hold the other viewpoint tend to focus on the separation region. Pipponiau et al.²⁰ suggested that the expansion/contraction of the separation bubble might be caused by the periodic shedding of vortices from the shear layer above the separation bubble. This mechanism involves a Kelvin-Helmholtz instability, providing a potential means by which the flow could be exploited for control purposes. An acoustic feedback loop²¹ or a global instability¹³ are also suggested as potential downstream sources of the unsteadiness. Recent research has indicated that the unsteadiness may have sources both upstream and downstream, with the strength of the interaction determining the relative magnitude of the dependence.^{22,23}

Localized Arc Filament Plasma Actuators (LAFPAs) were developed at The Ohio State University as a means to introduce strong, tailored, high frequency perturbations to flows.²⁴⁻²⁶ They have been explored as a noise mitigation and mixing enhancement technique in high-speed, high Reynolds number jets^{25,26} and recently for cavity flow control.²⁷ The flexibility of the LAFPAs also enables them to be used for feedback control.²⁸ The possibility of natural instabilities within SWBLIs which modify the separation size suggested that the ability of LAFPAs to mitigate SWBLI induced separation should be investigated. Titchener et al.²⁹ has observed that a single oblique SWBLI, or “unit problem” (see Figure 1), is probably not an adequate model of a supersonic inlet, however the goal of this research is to fundamentally explore the ability of LAFPAs to modify such a flow; therefore a unit problem was deemed an appropriate environment in which to conduct initial testing of the LAFPAs.

The separation control authority of the LAFPAs had previously shown to hold promise in a preliminary work.³⁰ The test facility was therefore improved and enlarged, and more extensive measurements were conducted.³¹ Further experiments concluded that when the LAFPAs are located upstream of the interaction region their primary effect is to shift the reflected shock upstream.³² It was suggested that the actuators were merely heating the incoming boundary layer, thereby degrading and enlarging the separation, displacing the reflected shock. This paper seeks to confirm this hypothesis through further analysis and experiment.

II. Experimental Methodology

A. Physical Arrangement

The facility in which the LAFPAs are tested models a single, oblique, impinging SWBLI. It is a blow-down facility with a freestream Mach number of 2.33. The air for the facility is compressed, dried and stored in two large tanks (~36 m³ total volume). The air supply is sufficient to run continuously, however other factors (tunnel temperature, oil buildup during PIV, etc.) typically limit a run to 1 to 2 minutes. The test section is rectangular, 76.2 mm by 72.9 mm, and the stagnation temperature is approximately ambient. There is optical access to the test section through two nominally 76 mm high by 250 mm long fused quartz windows. A narrow window in the test section ceiling allows for a laser sheet along the tunnel centerline. The primary shock is generated by a 10° compression ramp on the tunnel ceiling. The shock generator can be placed at three distinct streamwise locations, allowing the effective location of the LAFPAs to be varied. Figure 2 depicts the test section used in this work. It also shows the length scale, L , which is the nominal interaction length, and the normalized streamwise coordinate (X^*) used in this paper. For more details regarding the facility please refer to Webb et al.³¹

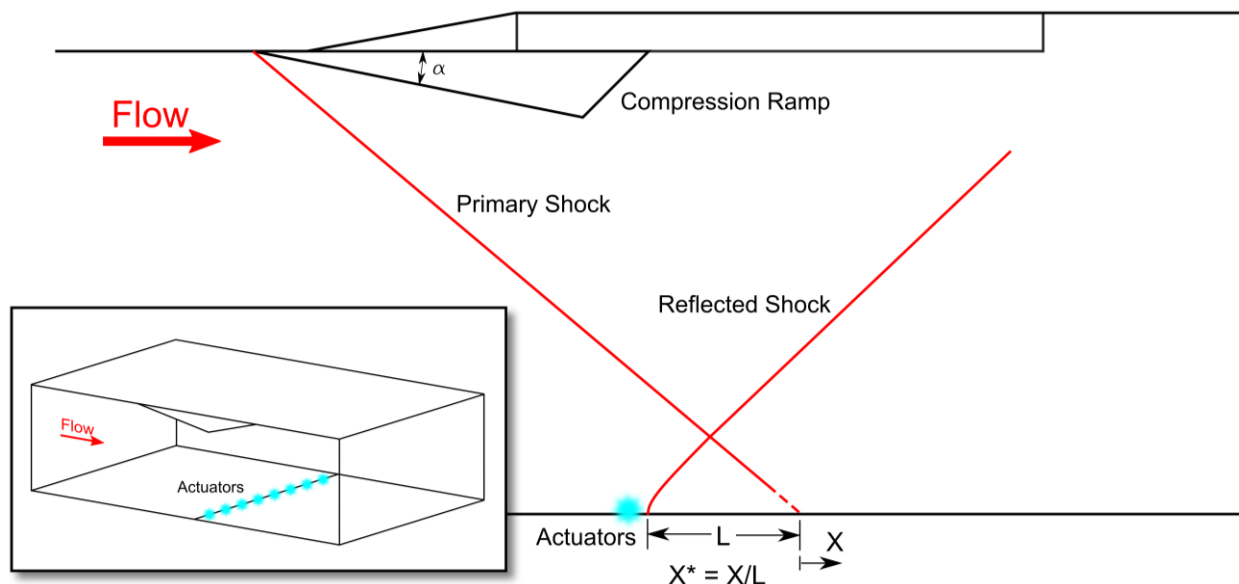


Figure 2: Test Section Schematic with Compression Ramp Model Installed; Inset Shows Spanwise Arrangement of the LAFPAs

The LAFPAs consist of two tungsten electrodes with the tips flush to the tunnel surface. The electrodes are 1 mm in diameter, and are in a groove 0.5 mm deep. The groove serves to shield and stabilize the arc after breakdown. Previous research has shown the groove to have a negligible effect on the control authority of the LAFPAs over

jets.³³ The electrode spacing is 3.5 mm (center-to-center) and 5.2 mm between actuators. As shown in the inset in Figure 2, there are eight actuators arranged in a spanwise row across the facility. For this work, the streamwise location of the row was varied throughout the upstream region of the interaction. The electrodes are also arranged in the spanwise line, so that the flow direction is across the gap between electrodes. Perturbations are generated by the formation of an arc between the electrodes, and the subsequent heat release. The power supply used in this work was developed at the Gas Dynamics and Turbulence Laboratory and allows discrete perturbations (breakdown, arc formation, then shutdown) to be generated continuously at frequencies up to 200 kHz.²⁴ The duty cycle (percent of the period for which the actuator is arcing) is variable up to 50%. Due to the goal of exploiting the flow to amplify the perturbations, rather than brute forcing of the flow, the actuators have a relatively low power deposition. Breakdown power is large, but the extremely short duration of the process results in a negligible contribution to the average power. The instantaneous power of the steady state arc is approximately 100 W, and the average power depends on the duty cycle. For the majority of this work the duty cycle was 50%, yielding an average power of 50 W per actuator, or 400 W overall. This is approximately 0.13% of the flow power ($P = \rho_\infty A U_\infty^3$).

B. Flow Diagnostics

Schlieren imaging was used as a fast and easy diagnostic for observing the flow density gradients, particularly the wave structure. This allowed the baseline flow to be confirmed as the desired flow. The interaction length (“L” in Figure 2) can also be measured from the schlieren images, and any changes in the wave structure due to actuation can be observed.

Particle Image Velocimetry (PIV) was performed using two distinct configurations. The first was two-component PIV on a streamwise-vertical plane along the tunnel centerline (subsequently referred to as “streamwise PIV”). This yielded quantitative data regarding the LAFPA’s ability to modify the centerline interaction. The second configuration was stereoscopic PIV on a streamwise-spanwise oriented plane located 2 mm above the floor (subsequently referred to as “horizontal PIV”). Figure 3 is a schematic of both PIV configurations. Only preliminary results have been collected in this configuration, however it allows the spanwise variation in the interaction to be examined as well as a better view of the separation region. Olive oil seed particles were introduced into the flow in the stagnation chamber using two particle atomizers in parallel. This setup yielded particles with a nominal diameter slightly less than 1 μm . The PIV data for both configurations were acquired using the commercially available DaVis 7.2 PIV software. The streamwise PIV data were collected using a single LaVision Imager Pro X camera; the horizontal PIV used two LaVision Imager Pro cameras. The laser was a Spectra Physics Quanta-Ray PIV 400 laser. DaVis was used to correlate and post-process the data, which were then transferred to MATLAB for analysis and reduction.

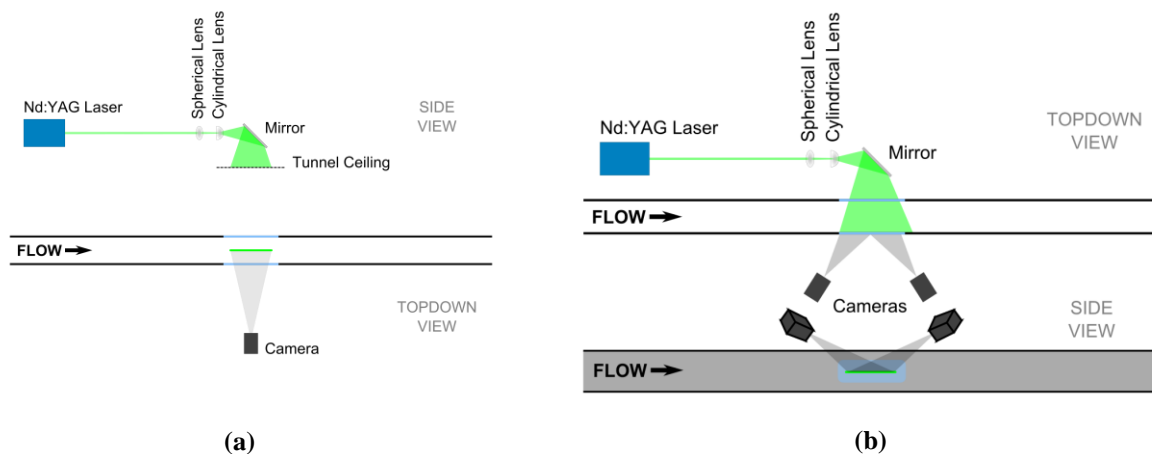


Figure 3: PIV Physical Configuration, a) Streamwise PIV, b) Horizontal PIV

III. Results and Discussion

A. Baseline Flow

The baseline flow of this facility has been extensively studied and found to conform well to the characteristics of SWBLIs documented in literature. Figure 4 is a long-exposure schlieren image of the baseline flow. The two dark lines are the incident and reflected shock waves. There are also several weak shocks present due to seams in the facility, which have been confirmed (with PIV) to have negligible effect on the flow. The interaction length, as defined in Figure 2, has been measured to be 39 mm. This length, in addition to being used to normalize streamwise locations, was also used to normalize the frequency of the low-frequency unsteadiness of the interaction region and the forcing frequencies. The unsteadiness frequency (and therefore potentially the most amplified frequencies) has been shown to vary between approximately 0.03 and 0.5 when normalized by the freestream velocity and the interaction length.¹⁵ The normalized low frequency associated with the reflected shock foot is $St = 0.03$.

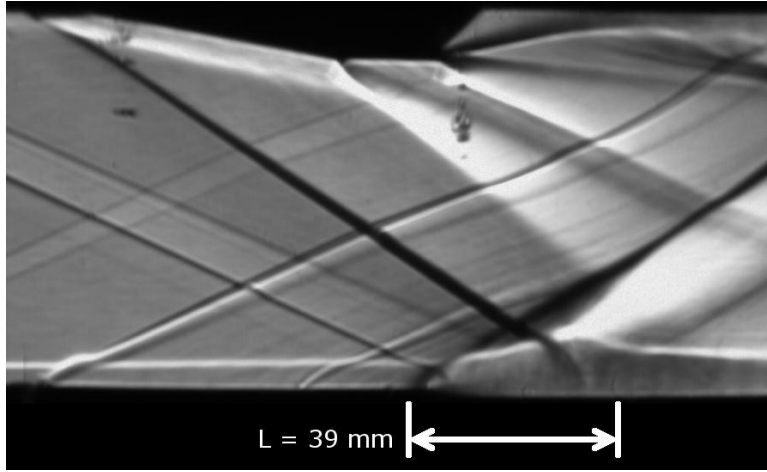


Figure 4: Baseline Long-Exposure Schlieren Image

As it was previously postulated that the LAFPAs are merely affecting the SWBLI through the upstream boundary layer³², and the nature of interaction depends on the state of the boundary layer,(pp. 28³⁴) characterization of the upstream boundary layer is important. Streamwise PIV data were used to document the upstream boundary layer, and Table 1 details the results. The boundary layer thickness (δ) is based on the $0.99U_\infty$ criterion. The integral quantities are calculated both in the compressible and incompressible manner (subscript “i” denotes “incompressible”). The density profile for the compressible quantities was estimated using the method proposed by Maise and McDonald.³⁵ Although these quantities may more accurately reflect the flow characteristics, the incompressible quantities are more widely used, and thus more easily comparable to literature.(pp. 21³⁴) Reynolds number based on several length scales is tabulated, but the most commonly used is that based on the incompressible momentum thickness.

Table 1: Upstream Boundary Layer Properties

M_∞	u_∞ (m/s)	δ (mm)	δ_i^* (mm)	θ_i (mm)	H_i	δ^*	θ (mm)	H
2.33	559	5.35	1.40	0.78	1.79	2.28	0.53	4.27
		Re (1/m)	Re$_\delta$	Re$_\theta$	Re$_{\theta_i}$			
		$35.7 \cdot 10^6$	191,000	18,900	27,900			

More information regarding the baseline flow can be obtained from Webb et al.³² In particular it is demonstrated that the incoming boundary layer is turbulent, the boundary layer separates, and the unsteadiness of the interaction is consistent with that observed in literature.

B. LAFPA Control Authority

The most obvious effect of the LAFPAs when located in and around the upstream end of the interaction is the displacement of the reflected shock upstream.³² This effect is most readily observed from velocity difference maps

constructed from streamwise PIV data by subtracting the baseline vector field from the forced vector field. The LAFPAs were initially located at $X_a^* = -0.83$, and operated in-phase at a frequency of $St_F = 0.03$. The results are shown in Figure 5. The reflected shock clearly moves upstream and the interaction region also moves slightly upstream. The reflected shock movement is clearly visible in the vertical velocity difference maps as a dark line (not to be mistaken for the shock thickness), therefore the streamwise velocity maps will be omitted.

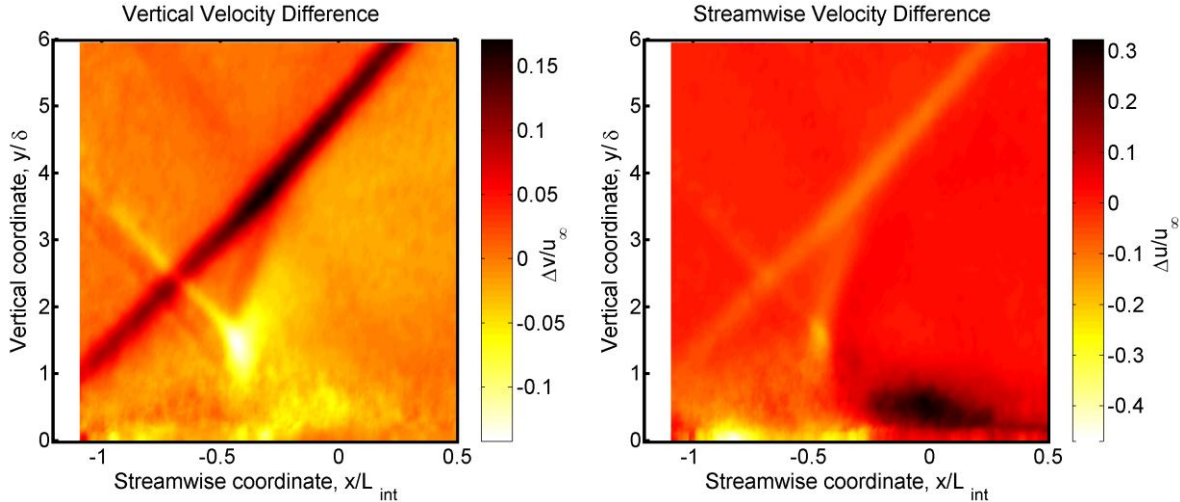
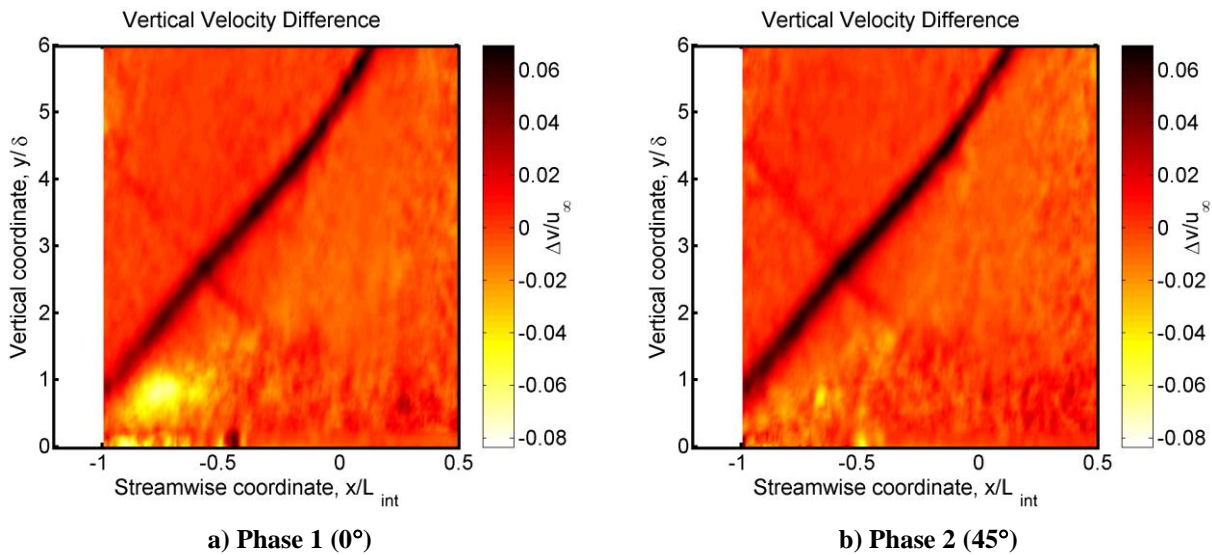


Figure 5: Ensemble-Averaged Velocity Difference Fields with Forcing Strouhal Number $St_F = 0.03$

In order to further investigate the LAFPAs' ability to displace the reflected shock, phase-locked PIV data were acquired. DaVis has the capability to synchronize acquisition with an external trigger signal. This feature was used to acquire the data at eight evenly spaced intervals throughout the LAFPAs' forcing period, providing insight into the interaction's phase-averaged behavior. The velocity difference map for each of these phases is shown in Figure 6. The phase is denoted by its angle, where 0° is when the LAFPAs begin arcing (Figure 6a), and 180° is when they cease arcing (Figure 6e). Examining Figure 6 shows that the reflected shock appears to travel upstream while the LAFPAs are arcing, and relax toward the baseline case after the arcing ceases. At this frequency, the shock does not appear to have sufficient time to relax completely back to the baseline. This would appear to support the previously hypothesized mechanism which regards the LAFPAs' heat addition as the primary control mechanism.



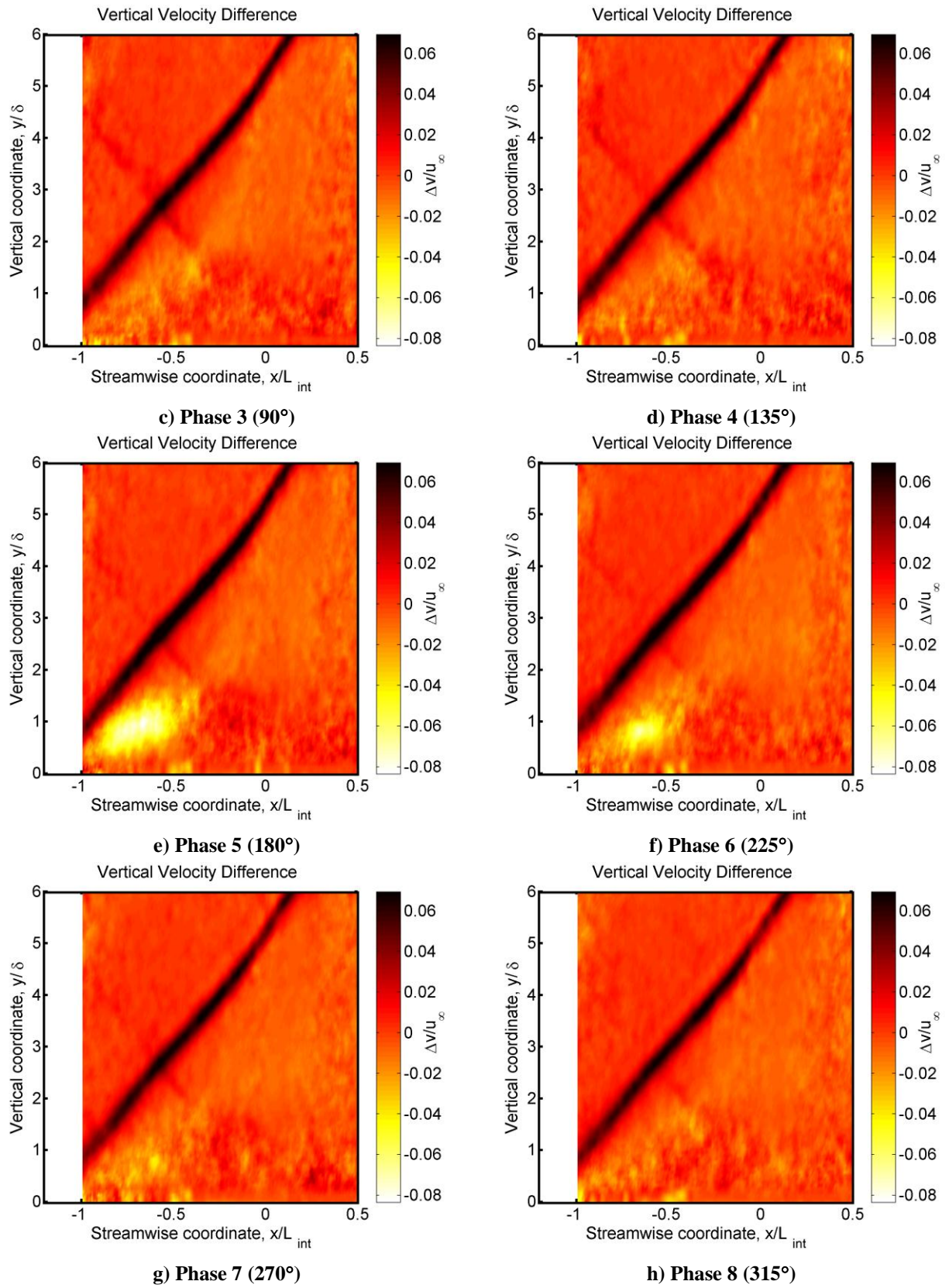
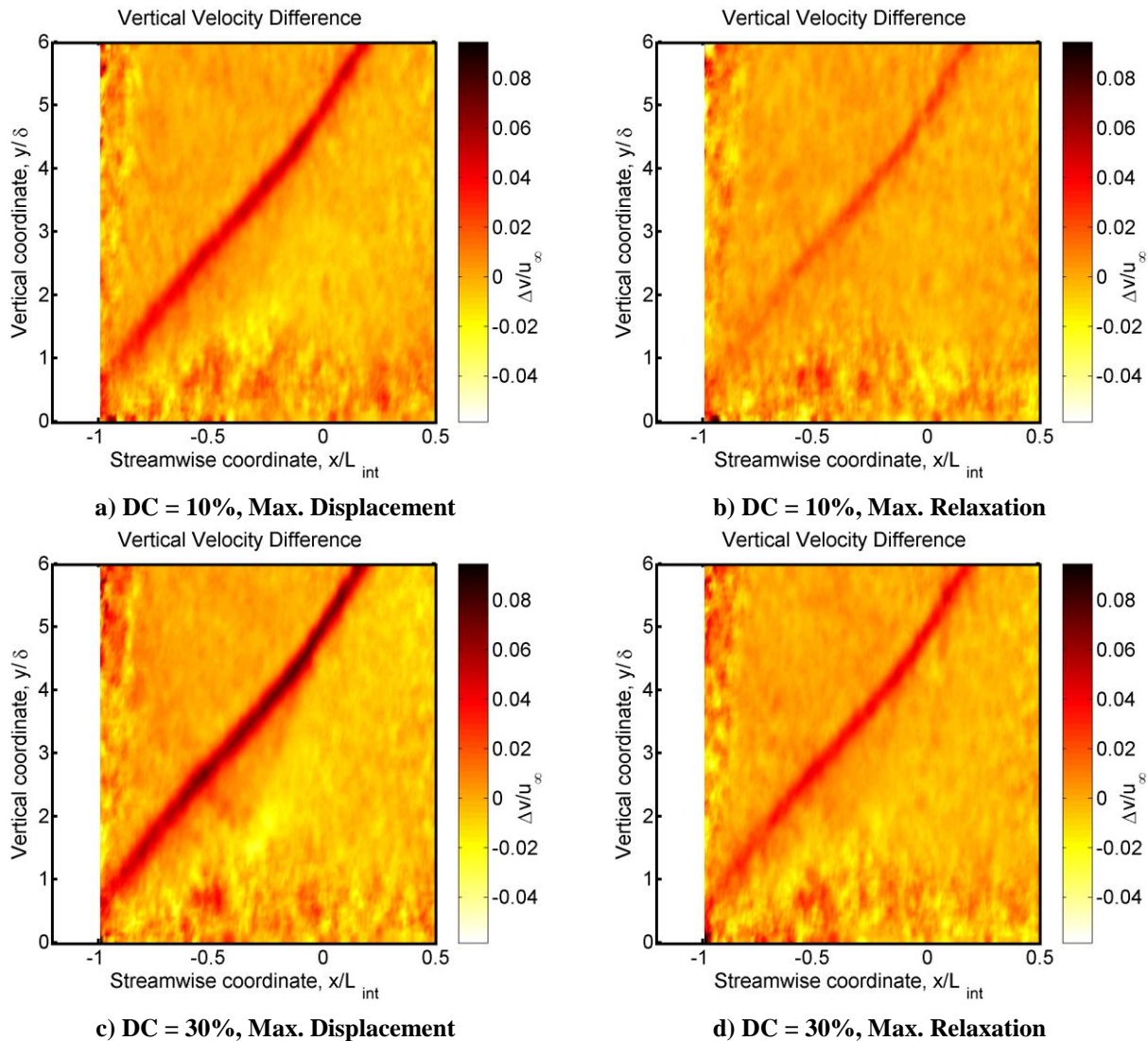


Figure 6: Ensemble-Averaged Velocity Difference Fields for $St_F = 0.03$ and $DC = 50\%$ Phase Sweep

If the primary control mechanism is through heating, then changing the duty cycle (time averaged power deposition) should have a strong effect on the reflected shock displacement. The actuators were therefore operated at duty cycles of 10%, 30%, and 50%, and the results are shown in Figure 7. As will be discussed later, it was determined that the streamwise location of the LAFPAs had a negligible effect on their control authority, therefore the LAFPAs were located at $X_a^* = -0.96$ for these experiments. The frequency of actuation was maintained at $St_F = 0.03$. Although eight phases were collected for each case, only two are displayed: the phase at which maximum shock displacement occurs (“Max. Displacement”) and that at which minimum shock displacement occurs (“Max. Relaxation”). The reflected shock displacement is seen to increase with increasing duty cycle for both phases. This supports the hypothesis that the LAFPAs exert their control authority through heating. A higher duty cycle indicates that the LAFPAs are arcing for a greater percentage of the period, which not only increases the amount of time the boundary layer is being heated, but also decreases the time in which the shock relaxes back to the baseline.



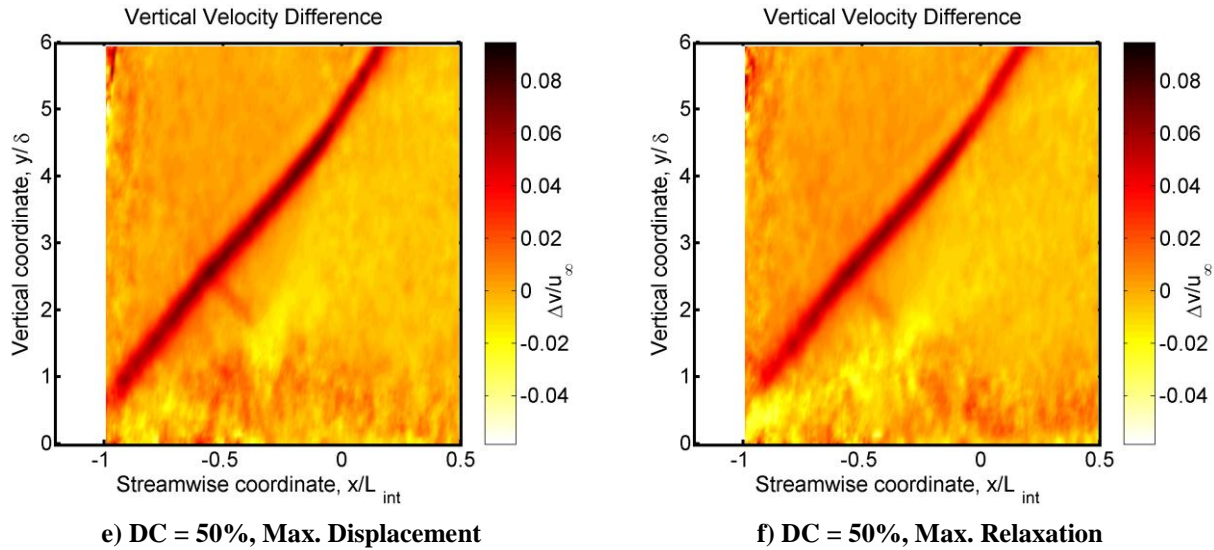


Figure 7: Ensemble Averaged Velocity Difference Fields for a Variety of Duty Cycles

In addition to examining the dependence of control authority on duty cycle, the effects of actuator location and operating frequency were investigated. It was found that within the region tested ($-1.09 \leq X^* \leq -0.77$), the location had a negligible effect on control authority. Instabilities often have receptivity regions, where introduced perturbations are most efficiently amplified. Thus, the lack of location dependence, near the expected receptivity region, coupled with the finding that there is no frequency at which effectiveness was maximized seems to indicate that the LAFPA's are not controlling the flow by manipulating an instability associated with the unsteadiness near the upstream end of the interaction. The nature of the dependence of the actuator's control authority on frequency also suggests that the time spent arcing, and perhaps more importantly the available relaxation time, is the important factor in determining the mean displacement amount. The complete results of the parameter sweep are published in Webb et al.³²

C. Further Investigation of Flow Control Mechanism

Previously the LAFPA's have manipulated natural instabilities to achieve control authority^{25,36} however, that does not appear to be the case for this configuration. This can be observed from the manner in which the LAFPA's control authority depends on location and frequency. Evidence from the phase and duty cycles sweeps suggests that the LAFPA's are simply heating the upstream boundary layer. Jaunet et al.³⁷ have observed that the reflected shock is displaced upstream if the surface beneath the incoming boundary layer is heated. The change in density was suggested as a potential reason for this displacement. Reducing the incoming boundary layer density alters the mass balance within the separation region causing the bubble to expand.³⁸ Their observed displacement is similar to what has been observed in this work; however, the magnitude of the effect is greater in their case. Boundary layer heating also accounts for the lack of control authority dependence on location (as long as the LAFPA's remain upstream of the interaction). As previously mentioned, both the effects of frequency and duty cycle trends are consistent with a heating mechanism. This hypothesis seems to be supported by observed trends in the current work, however, the relatively small power deposition by the LAFPA's, estimated to be almost two orders of magnitude less than that used by Jaunet et al.³⁷, makes the generation of such a substantial effect a dubious proposition. It is conceivable, however, that the high power density of the LAFPA's could enable them to produce the observed effect.

The large effect, relative to the size of the power input, prompted a more thorough investigation, despite clear evidence of a heating mechanism. Souverein³⁸ addresses the relationship between the displacement thickness, and the separation length. Although the presented relationships are somewhat complex, when all other parameters are held constant (as in this work), the relationship reduces to a proportionality between the displacement thickness and the separation length. This result is intuitive: a degraded turbulent boundary layer is less resistant to separation; therefore, the separation size will increase. In addition, since the actuators heat the flow, the upstream travelling pressure waves (in the subsonic region of the boundary layer) will travel upstream faster, causing the separation to expand upstream, thereby pushing the reflected shock upstream.

The results make sense; the question is merely one of scale: Can the LAFAPs produce a sufficient degradation to generate the observed displacement? For the initial test case ($St_F = 0.03$), the mean shock movement was approximately 4 mm (75% of the boundary layer thickness upstream of the interaction). The overall interaction length was measured to be 39 mm (see Figure 4) giving an increase of 10%. Assuming the shock movement (interaction length change) is caused by a separation expansion, the LAFAPs must be able to increase the incoming boundary layer displacement thickness by at least 10%. An initial, simplified analysis was conducted to determine if this is possible. The LAFAPs were assumed to operate strictly through Joule heating (increasing the total temperature). Quasi-one-dimensional, adiabatic, perfect gas flow was assumed, and the wall normal pressure gradient was assumed zero. The total temperature profile downstream of the LAFAPs was estimated using a basic knowledge of heat transfer and the known power deposition. The total temperature profile allows the density profile to be calculated, which, in combination with baseline velocity profile obtained through PIV, can be used to calculate the forced displacement thickness. Note that for both the baseline and forced displacement thicknesses, the compressible values were used. The effects of compressibility on density were estimated using the method proposed by Maise and McDonald.³⁵ Using the proportionality relation indicates that the LAFAPs can only increase the interaction length by 1.9 mm if they operate strictly through Joule heating, or they must output 0.84 kW to generate the observed effect. Comparing this to the actual 0.4 kW means that the LAFAPs cannot generate the observed effect through Joule heating alone.

Although Joule heating alone is insufficient to generate the observed effect, the LAFAPs also affect the velocity profile. Kleinman et al.³⁹ performed two-dimensional simulations of the LAFAPs in jet flow. These simulations found that significant mass injection from the groove takes place. Although expansion along the groove prevents the injection from being significant, a small amount of injection would still act to generate a wake, degrading the velocity profile. Hahn et al.³³ show that the groove has an insignificant effect on the LAFAPs' control authority, supporting the conclusion that injection has a minimal effect in this work.

It is however unlikely that the LAFAPs have no effect on the boundary layer velocity profile. This was one of the major assumptions of the earlier simplified analysis. In order to eliminate this assumption, experiments were conducted in which the undisturbed boundary layer was forced and velocity profiles were collected using PIV data. Two forcing frequencies: $f = 1$ kHz and 20 kHz were used. The duty cycle for both frequencies was 50%. Due to data corruption by the glow of the LAFAPs velocity profiles from $\sim 14\delta$ downstream were scaled to determine the effect of the LAFAPs on the velocity profile. It was unclear whether the displacement thickness or boundary layer thickness was the proper scaling parameter in this case. Therefore, both were used, and the resulting differences found to be negligible. When the experimental profiles were used, it was found that the estimated temperature profile necessary to generate the observed effect for the $f = 1$ kHz case required 0.4 kW, and for the $f = 20$ kHz, 0.38 kW. Thus this analysis showed that the LAFAPs can increase the displacement thickness sufficiently to result in the observed changes, further confirming the hypothesized mechanism.

The proposed control mechanism is that the actuators degrade the upstream boundary layer, resulting in an increased separation size, which displaces the reflected shock upstream. It has been shown that the LAFAPs are capable of increasing the displacement thickness sufficiently to accomplish the observed shock displacement. In order to further confirm this mechanism, preliminary horizontal PIV measurements were collected for baseline and forced cases, and the footprint of the separation region was examined. Figure 8 shows the streamwise velocity maps of the baseline and forced cases. Although the plane is only 2 mm from the surface, the separation region vertical dimension is small; therefore no mean reversed flow is detected at this location. However, the separation region is visible because of the shear layer over it, which is clearly captured in the measurements. An examination of the "separation" region shows that the actuators do enlarge the separation, resulting in the reflected shock being pushed upstream. This result can also be confirmed from the vertical velocity maps (not shown). It should be noted that the low velocity lines present in Figure 8 are merely due to plasma glow (\parallel on the left) and laser scatter (\perp on the right).

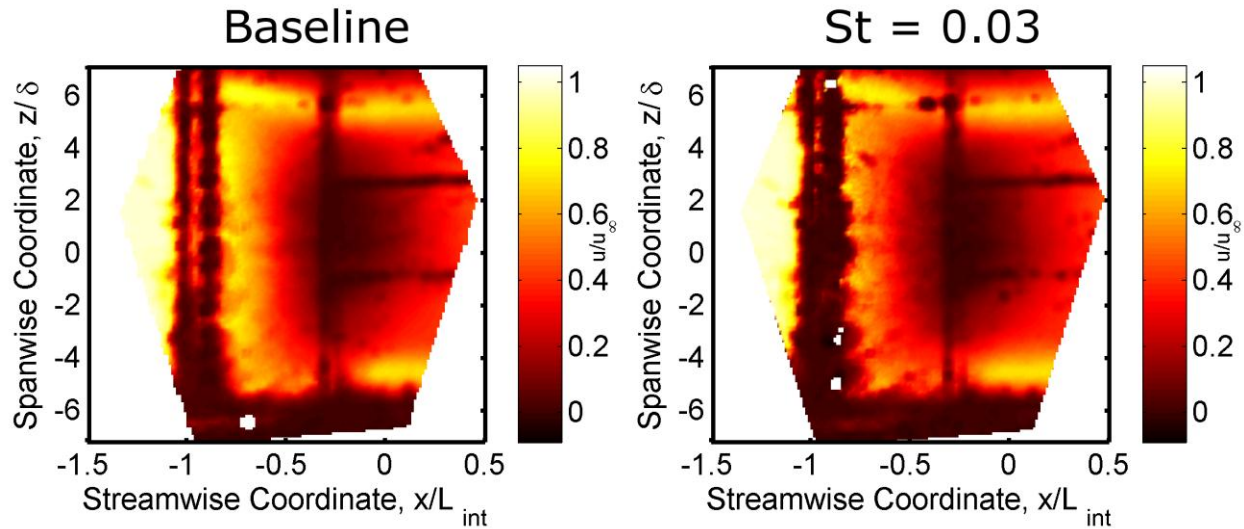


Figure 8: Baseline and Forced Horizontal PIV Streamwise Velocity Maps

The results show that the LAFPAs are most likely controlling the interaction through heating the boundary layer, which enlarges the separation, displacing the shock. Thus the LAFPAs are not manipulating natural instabilities in this configuration. However, in other configurations, namely with the LAFPAs downstream where they cannot modify the incoming boundary layer, they may be able to manipulate instabilities associated with the SWBLI. Increasing our understanding of the SWBLI dynamics is essential for optimally manipulating instabilities. One aspect of the dynamics, which has only recently been recognized as important is the interaction between the corner flows and the centerline. The preliminary PIV measurements are not high quality, and data near the walls is suspect. However these measurements are being improved, and when the quality is sufficient, they will be able to provide substantial data about how the LAFPAs affect the centerline/corners and how these two interplay. Of especial interest is to see how forcing with just the centerline, or just the sidewall actuators causes these regions to interact.

IV. Conclusions

The LAFPAs' control over a Mach 2.3, impinging, oblique SWBLI with a turbulent incoming boundary layer ($Re_{\theta_i} = 27,900$) has been investigated. The baseline flow has been observed to be consistent with what is described in literature.³² The LAFPAs were observed to displace the reflected shock upstream by approximately one boundary layer thickness (~ 5 mm). The results of phase-locked PIV measurements, as well as a parametric study led to the hypothesis that the LAFPAs were controlling the flow by heating the upstream boundary layer. Both the phase-locked PIV and the duty-cycle study suggested that the mechanism was dependent on the actuators arcing duration, rather than the frequency of actuation. The location and frequency studies lent weight to this conclusion by demonstrating that the LAFPAs were not controlling the flow through the manipulation of natural instabilities.

Forcing the undisturbed boundary layer, combined with further analysis has confirmed that the LAFPAs can generate the observed effect through boundary layer degradation. Horizontal PIV measurements confirming that the separation expands when the flow is forced further reinforces this conclusion. Therefore, it is concluded that in this configuration, the LAFPAs exert their control authority by a modification of the upstream boundary layer, primarily through heat addition. Future horizontal PIV measurements will be used to gain an improved understanding of the corner flow dynamics. Additional physical configurations (namely with the LAFPAs located in the downstream portion of the interaction) will also be examined to ascertain the LAFPA's effects in that arrangement.

Acknowledgments

The support of this work by the Air Force Office of Scientific Research (Dr. John Schmisser) is gratefully acknowledged.

References

- ¹ Syberg, J. and J. L. Koncsek, "Experimental Evaluation of an Analytically Derived Bleed System for a Supersonic Inlet," *Journal of Aircraft* Vol. 13, No. 10 (1976): 792-97.
- ² Baruzzini, D., "An Industry Perspective on the Role of Bleed in High-Speed Inlet Design Process," (2012): Private Communication
- ³ Shahneh, A. and F. Motallebi, "Effect of Submerged Vortex Generators on Shock-Induced Separation in Transonic Flow," *Journal of Aircraft* Vol. 46, No. 3 (2009): 856-63.
- ⁴ Anderson, B. H., J. Tinapple, and L. Surber, "Optimal Control of Shock Wave Turbulent Boundary Layer Interactions Using Micro-Array Actuation," *3rd AIAA Flow Control Conference*: 2006-3197.
- ⁵ Babinsky, H., Y. Li, and C. P. Ford, "Microramp Control of Supersonic Oblique Shock-Wave/Boundary-Layer Interactions," *AIAA Journal* Vol. 47, No. 3 (2009): 668-75.
- ⁶ Lee, S., M. Goettke, E. Loth, J. Tinapple, and J. Benek, "Microramps Upstream of an Oblique-Shock/Boundary-Layer Interaction," *AIAA Journal* Vol. 48, No. 1 (2010): 104-18.
- ⁷ Lee, S., E. Loth, and H. Babinsky, "Normal Shock Boundary Layer Control with Various Vortex Generator Geometries," *AIAA 5th Flow Control Conference*: 2010-4254.
- ⁸ Babinsky, H. and H. Ogawa, "Sbli Control for Wings and Inlets," *Shock Waves* Vol. 18, No. 2 (2008): 89-96.
- ⁹ Kalra, C. S., S. H. Zaidi, R. B. Miles, and S. O. Macheret, "Shockwave-Turbulent Boundary Layer Interaction Control Using Magnetically Driven Surface Discharges," *Experiments in Fluids* Vol. 50 (2011): 547-59.
- ¹⁰ Solomon, J. T., R. Kumar, and F. S. Alvi, "High-Bandwidth Pulsed Microactuators for High-Speed Flow Control," *AIAA Journal* Vol. 48, No. 10 (2010): 2386-96.
- ¹¹ Souverein, L. J. and J.-F. Debiève, "Effect of Air Jet Vortex Generators on a Shock Wave Boundary Layer Interaction," *Experiments in Fluids* Vol. 49 (2010): 1053-64.
- ¹² Narayanaswamy, V., L. Raja, and N. Clemens, "Characterization of a High-Frequency Pulsed-Plasma Jet Actuator for Supersonic Flow Control," *AIAA Journal* Vol. 48, No. 2 (2010): 297-305.
- ¹³ Toubert, E. and N. D. Sandham, "Large-Eddy Simulation of Low-Frequency Unsteadiness in a Turbulent Shock-Induced Separation Bubble," *Theoretical and Computational Fluid Dynamics* Vol. 23 (2009): 79-107.
- ¹⁴ Dolling, D. and L. Brusniak, "Separation Shock Motion in Fin, Cylinder, and Compression Ramp-Induced Turbulent Interactions," *AIAA Journal* Vol. 27, No. 6 (1989): 734-42.
- ¹⁵ Dupont, P., C. Haddad, and J. F. Debiève, "Space and Time Organization in a Shock-Induced Separated Boundary Layer," *Journal of Fluid Mechanics* Vol. 559 (2006): 255-77.
- ¹⁶ Andreopoulos, J. and K. C. Muck, "Some New Aspects of the Shock-Wave/Boundary-Layer Interaction in Compression-Ramp Flows," *Journal of Fluid Mechanics* Vol. 180 (1987): 405-28.
- ¹⁷ Beresh, S. J., N. T. Clemens, and D. S. Dolling, "Relationship between Upstream Turbulent Boundary-Layer Velocity Fluctuations and Separation Shock Unsteadiness," *AIAA Journal* Vol. 40, No. 12 (2002): 2412-22.
- ¹⁸ Ganapathisubramani, B., N. Clemens, and D. Dolling, "Low-Frequency Dynamics of Shock-Induced Separation in a Compression Ramp Interaction," *Journal of Fluid Mechanics* Vol. 636 (2009): 397-425.
- ¹⁹ Beresh, S. J., J. F. Henfling, R. W. Spillers, and B. O. M. Pruett, "Very-Large-Scale Coherent Structures in the Wall Pressure Field beneath a Supersonic Turbulent Boundary Layer," *49th AIAA Aerospace Sciences Meeting*: 2011-746.
- ²⁰ Piponniau, S., J. Dussauge, J. Debiève, and P. Dupont, "A Simple Model for Low-Frequency Unsteadiness in Shock-Induced Separation," *Journal of Fluid Mechanics* Vol. 629 (2009): 87-108.
- ²¹ Pirozzoli, S. and F. Grasso, "Direct Numerical Simulation of Impinging Shock Wave/Turbulent Boundary Layer Interaction at $M=2.25$," *Physics of Fluids A* Vol. 18 (2006): 1-17.
- ²² Narayanaswamy, V., "Investigation of a Pulsed-Plasma Jet for Separation Shock/Boundary Layer Interaction Control," Ph.D. Thesis. University of Texas at Austin, (2010): Print.
- ²³ Toubert, E. and N. D. Sandham, "Low-Order Stochastic Modelling of Low-Frequency Motions in Reflected Shock-Wave/Boundary-Layer Interactions," *Journal of Fluid Mechanics* Vol. 671 (2011): 417-65.
- ²⁴ Utkin, Y. G., S. Keshav, J.-H. Kim, J. Kastner, I. V. Adamovich, and M. Samimy, "Development and Use of Localized Arc Filament Plasma Actuators for High-Speed Flow Control," *Journal of Physics D: Applied Physics* Vol. 40, No. 3 (2007): 685-94.
- ²⁵ Samimy, M., J.-H. Kim, J. Kastner, I. Adamovich, and Y. Utkin, "Active Control of High-Speed and High-Reynolds-Number Jets Using Plasma Actuators," *Journal of Fluid Mechanics* Vol. 578, No. 1 (2007): 305-30.
- ²⁶ Samimy, M., J.-H. Kim, J. Kastner, I. Adamovich, and Y. Utkin, "Active Control of a Mach 0.9 Jet for Noise Mitigation Using Plasma Actuators," *AIAA Journal* Vol. 45, No. 4 (2007): 890-901.

- ²⁷ Yugulis, K., J. Gregory, and M. Samimy, "Control of High Subsonic Cavity Flow Using Plasma Actuators," *51st AIAA Aerospace Sciences Meeting*: Forthcoming.
- ²⁸ Sinha, A., K. Kim, J. Kim, A. Serrani, and M. Samimy, "Extremizing Feedback Control of a High-Speed and High Reynolds Number Jet," *AIAA Journal* Vol. 48, No. 2 (2010): 387-99.
- ²⁹ Titchener, N., H. Babinsky, and E. Loth, "Can Fundamental Shock-Wave/Boundary-Layer Interaction Research Be Relevant to Inlet Aerodynamics?," *50th AIAA Aerospace Sciences Meeting*: AIAA 2012-0017.
- ³⁰ Caraballo, E., N. Webb, J. Little, J.-H. Kim, and M. Samimy, "Supersonic Inlet Flow Control Using Plasma Actuators," *47th AIAA Aerospace Sciences Meeting*: 2009-924.
- ³¹ Webb, N., C. Clifford, and M. Samimy, "Preliminary Results on Shock Wave/Boundary Layer Interaction Control Using Localized Arc Filament Plasma Actuators," *41st AIAA Fluid Dynamics Conference*: 2011-3426.
- ³² Webb, N., C. Clifford, and M. Samimy, "Control of Oblique Shock Wave-Boundary Layer Interactions Using Plasma Actuators," *6th AIAA Flow Control Conference*: 2012-2810.
- ³³ Hahn, C., M. Kearney-Fischer, and M. Samimy, "On Factors Influencing Arc Filament Plasma Actuator Performance in Control of High Speed Jets," *Experiments in Fluids* Vol. 37, No. 5 (2011).
- ³⁴ Babinsky, H. and J. K. Harvey, *Shock Wave-Boundary-Layer Interactions*. New York, New York: Cambridge University Press, 2011. Print.
- ³⁵ Maise, G. and H. McDonald, "Mixing Length and Kinematic Eddy Viscosity in a Compressible Boundary Layer," *AIAA Journal* Vol. 6, No. 1 (1968): 73-80.
- ³⁶ Samimy, M., M. Kearney-Fischer, J.-H. Kim, and A. Sinha, "High-Speed and High-Reynolds-Number Jet Control Using Localized Arc Filament Plasma Actuators," *Journal of Propulsion and Power* Vol. 28, No. 2 (2012).
- ³⁷ Jaunet, V., J. F. Debiève, and P. Dupont, "Experimental Investigation of an Oblique Shock Reflection with Separation over a Heated Wall," *50th AIAA Aerospace Sciences Meeting*: AIAA 2012-1095.
- ³⁸ Souverein, L., "On the Scaling and Unsteadiness of Shock Induced Separation." IUSTI, (2010): Print.
- ³⁹ Kleinman, R. R., D. J. Bodony, and J. B. Freund, "Numerical Modeling of Plasma Actuators in High Speed Jets," *AIAA/CEAS 15th Aeroacoustics Conference*: 2009-3190.